MICRO-FLUID THROUGH ARAMID/CELLULOSE NANOCOMPOSITE MEMBRANES AND ITS FILTRATION EFFICIENCY

by

Kang LIU[a], Qi ZOU[a], Zhongwen LING[a], Yuqing LIU[a*], and Jinyou LIN[b,c*]

[a] National Engineering Laboratory for Modern Silk, College of Textile and Clothing Engineering, Soochow University, Suzhou, Jiangsu, China
[b] Shanghai Institute of Applied Physics, Chinese Academy of Sciences, Shanghai, China
[c] Key Laboratory of High Performance Fiber and Products, Ministry of Education, Donghua University,Shanghai, China

Original scientific paper
https://doi.org/10.2298/TSCI1804691L

The paper concerns micro scale flow in a membrane consisted of aramid nanofibers and cellulose nanofibers via layer-by-layer technique. Surface morphology, surface wettability, and filtration performance are experimentally studied to elucidate the basic micro-fluid properties. The effect of the thickness on filtration efficiency is theoretically analyzed, and the paper concludes that the membrane is extremely effect to remove nanoparticles.

Key words: *aramid nanofibers, cellulose nanofibers, composite membranes, theoretical analysis, liquid filtration*

Introduction

In recent years, with the rapid development of the semiconductor industry, heavy metal ions in industrial wastewater have become a major source of pollution in water courses. Reductions in the content of heavy metal ions in wastewater and improvements to the environment have become focal points in the field of water treatment [1, 2]. Recently, electrospun nanofibrous membranes have been developed as an efficient method for liquid filtration [3-5]. Aramid nanofiber (ANF) membranes contain small diameter fibers and exhibit a large specific surface area [6]. This enables ANF to effectively filter ions with a diameter of less than 100 nm from water. Using the electrospinning method, cellulose nanofibers (CNF) can be produced following hydrolysis of cellulose acetate (CA) [7]. The resulting cellulose nanomembranes are hydrophilic and have a large specific surface area [8]. In this reported study, CNF were coated with ANF to produce a composite membrane material via the layer-by-layer (LBL) technique. This composite membrane exhibited high strength and hydrophilicity with a filtration efficiency of 98% for Fe_3O_4 which has a molecular diameter of 10 nm. In addition to experimental work, performance predictions of the membranes were calculated using classical filtration theories and the results were compared with the experimental results. The comparison suggested that there is a need for modifications in the modeling of the filtration capture performance of nanocomposite membranes for nanoparticles.

* Corresponding author's, e-mail: shliuyq@163.com, jinyoulin82@gmail.com

Empirical correlation between filtration efficiency and thickness of the composite membrane

The filtration efficiency, E, of a membrane, is defined:

$$E = \left[1 - \left(\frac{C_{\text{filtration}}}{C_{\text{feed}}}\right)\right] \cdot 100\% \tag{1}$$

where C_{feed} and $C_{\text{filtration}}$ are concentrations of feed and filtrate solutions.The filtration efficiency can be calculated using eq. (2), where A_{feed} and $A_{\text{filtration}}$ are the absorbance of feed and filtrate solutions [9]:

$$E = \left[1 - \left(\frac{A_{\text{filtration}}}{A_{\text{feed}}}\right)\right] \cdot 100\% \tag{2}$$

The quality factor, Q_{f}, is defined:

$$Q_{\text{f}} = -\frac{\ln(1-\eta)}{\Delta p} \tag{3}$$

where Δp is the pressure drop across the filter, and Q_{f} – the ratio between filtration efficiency and pressure drop [10]. A filter that has a high filtration efficiency and a low pressure drop will have high Q_{f}. Thus, a good quality filter will have a large Q_{f}. Also, η is equivalent to the E in eq. (1).

Carman [11] developed a mathematical theory for predicting the collection efficiency of fibrous filters in a continuous flow regime. In addition, these authors obtained an expression for pressure drop and particle collection efficiency of a fibrous medium. A filter's pressure drop is a function of solution viscosity, μ, filter thickness, L, sphericity, ϕ_{s}, velocity, V_0, fiber diameter, d_p, and material's porosity, δ, expressed:

$$\frac{\Delta p}{L} = \frac{180 V_0 \mu}{\phi_{\text{s}}^2 d_{\text{p}}^2} \frac{(1-\delta)^2}{\delta^3} \tag{4}$$

Experimental methods

The preparation of the ANF was conducted according to a previous publication [12]. In brief, 0.5 g of Kevlar yarns (DuPont Company) and 0.75 g of KOH were added to 250 ml of dimethylsulfoxide (DMSO). After a magnetically stirring this solution for one week at room temperature a dark-red DMSO dispersion of ANF was obtained. This solution was used to prepare ANF using electrospinning.

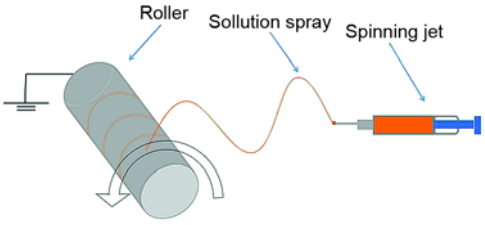

Figure 1. Electrospinning device

The electrospinning device used to prepare the ANF is shown in fig. 1. An acetic acid/acetone/DMAC (dimethylacetamide) mixture was used to adjust the necessary consistency of the solution, which was then injected into the syringe. The diameter of the syringe needle was 0.5 mm and spinning fluid flow was 0.5 mL/h. The receiving distance was 18 cm and the spinning voltage was 12 KV. The resulting

fibrous film was cut into of 20 × 20 cm square samples and these were soaked in NaOH for a week. The resulting film was rinsed of excess NaOH and then dried in air for later use.

It has been reported that the ANF can be dispersed and ionized in negatively charged polar solutions [12]. Yuan *et al.* [13] showed that the LBL self-assembly process can be used for the preparation of composite membranes. Therefore, the negatively charged ANF can self-assemble on the surface of CNF to form composite membranes. To obtain a positively charged substrate, the CNF were dipped into a 1 wt.% poly-diallyldimethylammonium chloride (PDDA) solution and then the CNF were washed with deionized (DI) water to remove the excess positive charges. After drying, the CNF were dipped into the ANF/DMSO solution to adsorb the negatively charged ANF. Subsequently, another rinsing with DI water was done to eliminate the excess negative charges before drying. After a full drying process, a stable, composite ANF/CNF membrane was obtained. After repeating the step for 2, 4, and 6 times, the CNF-2, CNF-4, and CNF-6 were prepared.

The structure of ANF/CNF composite membranes were characterized using a field emission SEM (S-4800). The water contact angle (WCA) of composite membranes was determined by the sessile drop method using a DataPhysicsDSA100 (Germany) contact angle measuring device. Optical absorption spectra of the feed solution and filtrate were measured using a UV-VIS spectroscopy (TU-1810) at room temperature.

Results and discussion

Table 1 summarizes the physical parameters of the CNF substrate with the ANF nanofiber coating. The substrate was fabricated by electrospinning and the nanofiber layers were obtained by the dispersion of DMSO. Samples ANF-2, ANF-4, ANF-6 were fabricated with different layers, producing membranes with different thicknesses. The mean fiber diameter, d_f, was estimated from the SEM examination of the membranes.

Table 1. Physical parameters of the CNF substrate and the ANF/CNF composites

Medium	Substrate	ANF-2	ANF-4	ANF-6
Fiber diameter d_f [nm]	535	18	18	18
Thickness $L \pm \Delta L$ [10^{-6}m]	12.5±0.5	0.25±0.03	0.55±0.05	0.86±0.05
Porosity [%]	42	75	75	75

Figure 2(a) shows the SEM micrographs of the SEM of CNF which reveals their morphology. As shown, the ANF were freely crisscrossed and their length was about 5 μm to 10 μm. Figure 2(b) shows the SEM of ANF membrane surface. Here, the aramid fiber membrane has a larger specific surface area, high porosity rendering it more advantageous for filtration tests [14]. The surface of composite appeared to be smooth, with the fibers exhibiting similar diameters and there was no bead structure or ribbon fiber production. Figure 2(c) shows that the CNF were covered by two-layer of ANF. Figure 2(d) shows a four-layered ANF membrane covering the CNF film. Figure 2(e) shows the six-layers of ANF coated on the CNF. Figure 2(f) shows the cross section diagram of the composite.The surface wettability of the initial CNF and prepared ANF/CNF composite membranes is depicted in fig. 3(a) which shows the WCA of CNF-2, CNF-4, and CNF-6. From the pictures, it is apparent that the CNF displayed hydrophilic performance, because the cellulose molecules contained a large number of hydroxyl groups. There were hydrogen bonds between the molecular chains as well as strong hydrogen bonds within the molecular chains.

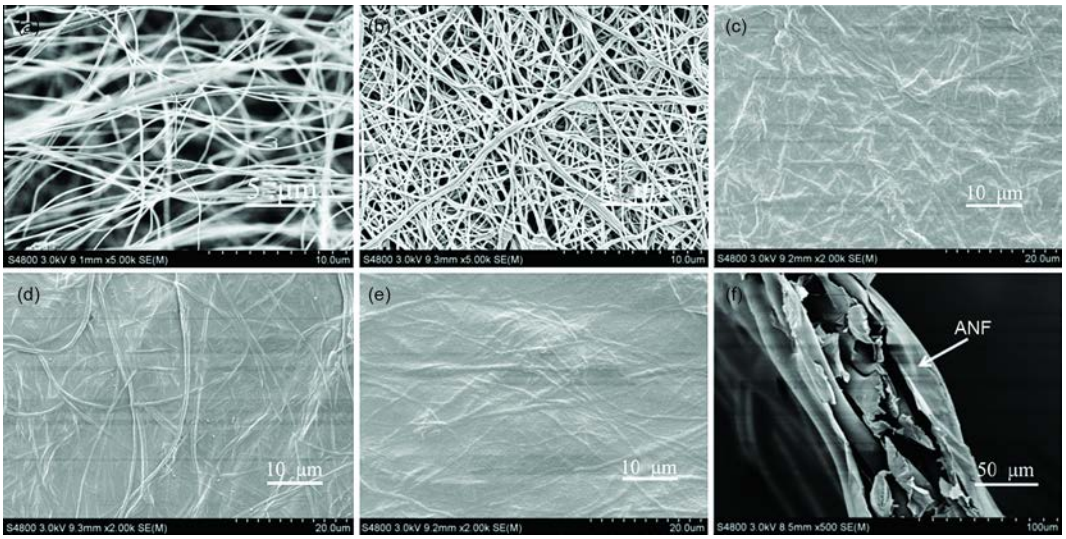

Figure 2. (a) the SEM image of CNF, (b) the SEM image of ANF membrane, (c) the SEM image of CNF-2, (d) the SEM image of CNF-4, (e) the SEM image of CNF-6, (f) the SEM of ANF/CNF membranes

The contact angle of the ANF/CNF composites increased with the number of layers of ANF in the composite, which appeared to enhance the hydrophilicity of the membrane. However, the hydrophilicity of composite membrane was inferior to the CNF, because of the presence of the pure hydroxyl groups in the CNF which exhibited higher hydrophilicity than the ANF's amide linkage. The ANF/CNF composite membranes were expected to be suitable for filter testing, because of their good hydrophilicity.

Figure 3(b) shows infrared spectra of the CNF and ANF/CNF. The results show that compared to CA, the infrared absorption peaks of CNF decreased at the 1725 per cm and 1370 per cm due to the hydrolysis of acetyl radical. Comparing CNF with ANF/CNF, the absorption peak of at 2885 per cm and 886 per cm was attributed to the C-H vibrations, while the vibration absorption peak of C-O-O was observed at 1640 per cm. The ANF/CNF has the characteristic peak of N-H vibration at 3326 per cm, which shows that the ANF successfully adhered to the CNF.

Figures 4(a)-4(c) show the UV-VIS spectra of the feed solution containing 10 nm Fe_3O_4 nanoparticles, the DI water and the filtered solution that had permeated through the ANF-2, ANF-4, and ANF-6. The initial solution contained Fe_3O_4 and its color was dark red. After being filtered, the solution became very clear indicating that the iron oxide had been removed from solution by the membrane. The composite membrane exhibited good filtering performance, probably due to the large surface of the ANF/CNF membrane The hydrogen bonding in the molecular structure helped to form a similar mesh structure cage molecular [15], which obstructed Fe_3O_4 particles from reaching the membrane surface. The SEM micrograph of the composite membrane surface is exhibited in fig. 4(f). Figure 4(d) illustrates the filtration performance of the membrane. The filtration efficiencies of CNF-2, CNF-4, and CNF-6 were approximately 94.7%, 96.9%, and 98.1%. The filtration efficiency was directly related to the thickness of nanofiber layer. Two to six layers of the ANF material were stacked onto the CNF substrate to form a nanofiber layer with the same porosity, but with an in-

creased thickness. The filtration results demonstrated that as the thickness of the ANF layer was increased, the filtration efficiency of the composite membrane improved.

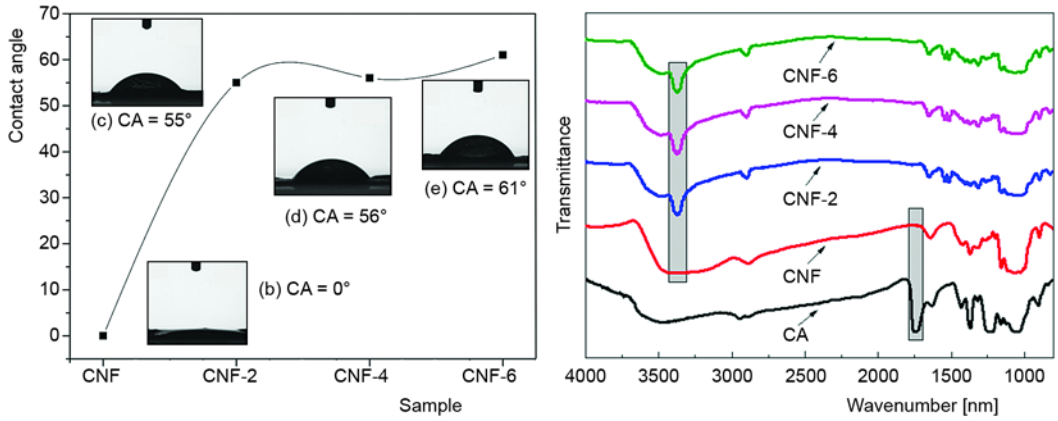

Figure 3. (a) The WCA of CNF, CNF-2, CNF-4, and CNF-6 (b) infrared absorption spectra of CNF and ANF/CNF

The filtration efficiency and pressure drop across a filter are represented by η and ΔP, as depicted in eq. (3). The pressure drop across the membrane is a function of solution viscosity, μ, filter thickness, L, sphericity, ϕ_s, velocity, V_0, fiber diameter, d_p, and material's porosity, δ as expressed in eq. (4). From this expression we can obtain the new equation, which describes the non-linear correlation between the filtration efficiency and thickness:

$$\frac{\ln(1-\eta)}{Q_f} = -\frac{180V_0\mu}{\phi_s^2 d_p^2}\frac{(1-\delta)^2}{\delta^3} \times L \tag{5}$$

Figure 4(e) shows the theoretic filtration efficiency as a function of the membrane different thickness, as expressed by eq. (5). The dotted part of the curve approximates the experimental results shown in fig. 4(d). However, the theoretical and experimental filtration efficiency results for the composite membranes that contained nanofiber layers were compared to determine the deviations between the two. It was found that the model equation accurately predicted the filtration efficiency of the membranes for the iron oxide nanoparticles. Hence, the model appeared to confirm that the nanofiber layer in the composite membrane improved the nanoparticulate filtration of the membrane.

Conclusion

In summary, ANF/CNF nanofiber composite membranes are a new type of environmentally friendly, water treatment membrane. The demonstarted filtration performance of these new membranes appear to make them suitable for water treatment. The thickness of the nanofiber layer in the membrane on the material's filtration performance was investigated. Experimental and theoretical results showed that the filtration efficiency of the composite was enhanced as the thickness of the nanofiber layer was increased. However, further study is

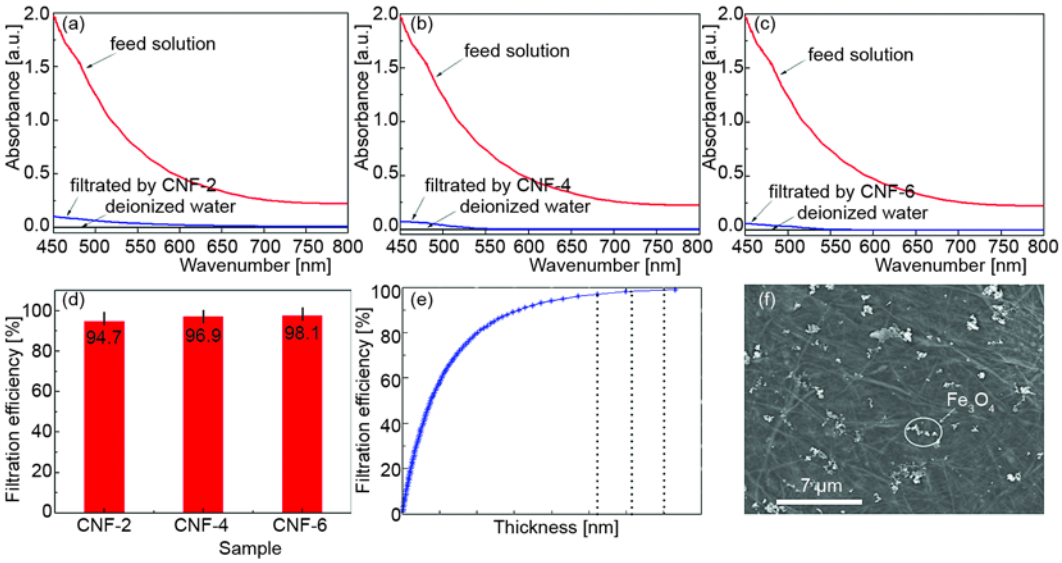

Figure. 4 (a)-(c) The UV-VIS spectra of 10 nm Fe_3O_4 feed solution, the DI water and the filtrate permeated through the CNF-2, CNF-4, CNF-6, (d) experimental filtration efficiency of the composite membranes, (e) theoretical filtration efficiency of the composite membranes, (f) the SEM of the composite surface

needed to determine how to further improve in the preparation of these composite membranes. This report is a potential, valuable foundation for further research on these new membranes.

Acknowledgment

The work is supported by a grant from National Natural Science Foundation of China, 51303200; Natural Science Foundation of Jiangsu province, BK2012196; Natural Science Foundation of Higher Education of Jiangsu Province of China, 14KJB320013.

References

[1] Haider, S., *et al.*, Preparation of the Electrospun Chitosan Nanofibers and their Applications to the Adsorption of Cu(II) and Pb(II) Ions From an Aqueous Solution, *Journal of Membrane Science, 328* (2009), 1-2, pp. 90-96
[2] Chauhan, G. S., *et al.*, Functionalization of Pine Needles by Carboxymethylation and Network Formation for Use as Supports in the Adsorption of Cr 6+, *Carbohydrate Polymers, 70* (2007), 4, pp. 415-421
[3] Gopal, R., *et al.*, Electrospun Nanofibrous Polysulfone Membranes as Pre-Filters: Particulate Removal, *Journal of Membrane Science, 289* (2007), 1-2, pp. 210-219
[4] Aussawasathien, D. C., *et al.*, Separation of Micron to Sub-Micron Particles from Water: Electrospun Nylon-6 Nanofibrous Membranes as Pre-Filters, *Journal of Membrane Science, 315* (2008), 1-2, pp. 11-19
[5] Li, X. W., *et al.*, Study on Highly Filtration Efficiency of Electrospun Polyvinyl Alcohol Micro-Porous Webs, *Indian Journal of Physics, 89* (2014), 2, pp. 175-179
[6] Yang, M., *et al.*, Dispersions of Aramid Nanofibers: a New Nanoscale Building Block, *Acs Nano, 5* (2011), 9, pp. 45-54
[7] Liu, Z., *et al.*, Needle-Disk Electrospinning Inspired by Natural Point Discharge, *Journal of Materials Science, 52* (2016), 4, pp. 1823-1830

[8] Ma, J., *et al.,* Highly Carbonylated Cellulose Nanofibrous Membranes Utilizing Maleic Anhydride Grafting for Efficient Lysozyme Adsorption, *Acs Applied Materials & Interfaces*, *7* (2015), 28, pp. 15658-15666
[9] Therefore, *et al.*, Electrospun Carbon Nanofiber Membranes for Filtration of Nanoparticles from Water, *Journal of Nanomaterials*, *2015* (2015), ID 247471
[10] Leung, W. F., *et al.,* Effect of Face Velocity, Nanofiber Packing Density and Thickness on Filtration Performance of Filters with Nanofibers Coated on a Substrate, *Separation & Purification Technology*, *71* (2010), 1, pp. 30-37
[11] Carman, P. C., *Flow of Gases through Porous Media*, Butterworths Scientific Publications, Oxford, UK, 1956
[12] Yang, M., *et al.*, Dispersions of Aramid Nanofibers: a New Nanoscale Building Block, *Acs Nano*, 5 (2011), 9, pp. 45-54
[13] Yuan, Y., *et al.*, Layer-by-Layer Self-Assembly of Aramid Nanofibers on Nonwoven Fabric for Liquid Filtration, *Polymer Composites*, On-line (2016), https://doi.org/10.1002/pc.24224
[14] Zhao, X. Y., *et al.*, Preparation and Property Study of PHBV/PVA Composite Membranes, *Applied Chemical Industry*, *7* (2013), pp. 1185-1188
[15] Srinivasa, P. C., *et al.,* Effect of Plasticizers and Fatty Acids on Mechanical and Permeability Characteristics of Chitosan Films, *Food Hydrocolloids*, *21* (2007), 7, pp. 1113-1122

Paper submitted: March 15, 2016
Paper revised: May 20, 2017
Paper accepted: July 20, 2017

© 2018 Society of Thermal Engineers of Serbia.
Published by the Vinča Institute of Nuclear Sciences, Belgrade, Serbia.
This is an open access article distributed under the CC BY-NC-ND 4.0 terms and conditions.